




ARE YOU A  
**SCIENTIFIC  
REBEL?**



Unleash your true potential  
with the new **CytoFLEX LX**  
Flow Cytometer

DARE TO EXPLORE



This information is current as  
of August 17, 2017.

## mTOR Signaling Inhibition Modulates Macrophage/Microglia-Mediated Neuroinflammation and Secondary Injury via Regulatory T Cells after Focal Ischemia

Luokun Xie, Fen Sun, Jixian Wang, XiaoOu Mao, Lin Xie,  
Shao-Hua Yang, Dong-Ming Su, James W. Simpkins, David  
A. Greenberg and Kunlin Jin

*J Immunol* published online 14 May 2014  
<http://www.jimmunol.org/content/early/2014/05/14/jimmunol.1303492>

---

<b>Supplementary Material</b>	<a href="http://www.jimmunol.org/content/suppl/2014/05/14/jimmunol.1303492.DCSupplemental">http://www.jimmunol.org/content/suppl/2014/05/14/jimmunol.1303492.DCSupplemental</a>
<b>Subscription</b>	Information about subscribing to <i>The Journal of Immunology</i> is online at: <a href="http://jimmunol.org/subscription">http://jimmunol.org/subscription</a>
<b>Permissions</b>	Submit copyright permission requests at: <a href="http://www.aai.org/About/Publications/JI/copyright.html">http://www.aai.org/About/Publications/JI/copyright.html</a>
<b>Email Alerts</b>	Receive free email-alerts when new articles cite this article. Sign up at: <a href="http://jimmunol.org/alerts">http://jimmunol.org/alerts</a>



# mTOR Signaling Inhibition Modulates Macrophage/Microglia-Mediated Neuroinflammation and Secondary Injury via Regulatory T Cells after Focal Ischemia

Luokun Xie,\* Fen Sun,\* Jixian Wang,\*<sup>†</sup> XiaoOu Mao,<sup>‡</sup> Lin Xie,<sup>‡</sup> Shao-Hua Yang,\* Dong-Ming Su,\* James W. Simpkins,\*<sup>§</sup> David A. Greenberg,<sup>‡</sup> and Kunlin Jin\*

Signaling by the mammalian target of rapamycin (mTOR) plays an important role in the modulation of both innate and adaptive immune responses. However, the role and underlying mechanism of mTOR signaling in poststroke neuroinflammation are largely unexplored. In this study, we injected rapamycin, a mTOR inhibitor, by the intracerebroventricular route 6 h after focal ischemic stroke in rats. We found that rapamycin significantly reduced lesion volume and improved behavioral deficits. Notably, infiltration of  $\gamma\delta$  T cells and granulocytes, which are detrimental to the ischemic brain, was profoundly reduced after rapamycin treatment, as was the production of proinflammatory cytokines and chemokines by macrophages and microglia. Rapamycin treatment prevented brain macrophage polarization toward the M1 type. In addition, we also found that rapamycin significantly enhanced anti-inflammation activity of regulatory T cells (Tregs), which decreased production of proinflammatory cytokines and chemokines by macrophages and microglia. Depletion of Tregs partially elevated macrophage/microglia-induced neuroinflammation after stroke. Our data suggest that rapamycin can attenuate secondary injury and motor deficits after focal ischemia by enhancing the anti-inflammation activity of Tregs to restrain poststroke neuroinflammation. *The Journal of Immunology*, 2014, 192: 000–000.

Stroke is the fourth leading cause of death and the leading cause of disability in the United States (1). Despite tremendous progress in understanding the pathophysiology of ischemic stroke, translation of this knowledge into effective therapies has largely failed. Systemic thrombolysis with recombinant i.v. tissue plasminogen activator remains the only treatment proven to improve clinical outcome of patients with acute ischemic stroke (2). However, because of an increased risk of hemorrhage beyond a few hours poststroke, only ~1–2% of stroke patients can benefit from recombinant i.v. tissue plasminogen activator (3, 4).

Molecular and cellular mediators of neuroinflammatory responses play critical roles in the pathophysiology of ischemic stroke, exerting either deleterious effects on the progression of tissue damage or beneficial roles during recovery and repair (5). Therefore, postischemic neuroinflammation may provide a novel

therapeutic approach in stroke. However, several therapeutic trials targeting neuroinflammatory response have failed to show clinical benefit (6). The cause remains unknown. However, targeting a single cell type or single molecule may not be an adequate clinical strategy. In addition, the biphasic nature of neuroinflammatory effects, which amplify acute ischemic injury but may contribute to long-term tissue repair, complicates anti-inflammatory approaches to stroke therapy.

Mammalian target of rapamycin (mTOR) is a critical regulator of cell growth and metabolism that integrates a variety of signals under physiological and pathological conditions (7, 8). Rapamycin is a Food and Drug Administration–approved immunosuppressant being used to prevent rejection in organ transplantation. Recent data show that mTOR signaling plays an important role in the modulation of both innate and adaptive immune responses (9). In experimental stroke, rapamycin administration 1 h after focal ischemia ameliorated motor impairment in adult rats (10) and in neonatal rats (11) and improves neuron viability in an in vitro model of stroke (12). However, the mechanisms underlying mTOR-mediated neuroprotection in stroke are unclear. In addition, stroke patients often experience a significant delay between the onset of ischemia and initiation of therapy. So it is important to determine whether rapamycin can protect from ischemic injury when administered at later time points.

In this study, we found that rapamycin administration 6 h after focal ischemia significantly reduced infarct volume and improved motor function after stroke in rats. In addition,  $\gamma\delta$  T cells and neutrophil infiltration were decreased, regulatory T cell (Treg) function was increased, and proinflammatory activity of macrophages and microglia was reduced in the ischemic hemispheres. Tregs from rapamycin-treated brains effectively inhibited proinflammatory cytokine and chemokine production by macrophages and microglia. Our data suggest that rapamycin attenuates secondary injury and motor deficits after focal ischemia by modulating poststroke neuroinflammation.

\*Department of Pharmacology and Neuroscience, Institute for Aging and Alzheimer's Disease Research, University of North Texas Health Science Center, Fort Worth, TX 76107; <sup>†</sup>Department of Neurology, Ruijin Hospital, Shanghai Jiao Tong University School of Medicine, Shanghai 200025, China; <sup>‡</sup>Buck Institute for Research on Aging, Novato, CA 94945; and <sup>§</sup>Department of Physiology and Pharmacology, Center for Neuroscience, Health Science Center, West Virginia University, Morgantown, WV 26506

Received for publication December 31, 2013. Accepted for publication April 11, 2014.

This work was supported by Public Health Service Grants NS57186 and AG21980 (to K.J.) and NS054687 and NS054651 (to S.-H.Y.).

Address correspondence and reprint requests to Dr. Kunlin Jin, Department of Pharmacology and Neuroscience, University of North Texas Health Science Center, 3500 Camp Bowie Boulevard, Fort Worth, TX 76107. E-mail address: kunlin.jin@unthsc.edu

The online version of this article contains supplemental material.

Abbreviations used in this article: ECA, external carotid artery; iNOS, inducible NO synthase; I/R, ischemia/reperfusion; MCAO, middle cerebral artery occlusion; mTOR, mammalian target of rapamycin; Q-RT-PCR, quantitative RT-PCR; Treg, regulatory T cell.

Copyright © 2014 by The American Association of Immunologists, Inc. 0022-1767/14/\$16.00

## Materials and Methods

### Focal cerebral ischemia

Transient focal cerebral ischemia was induced using the suture occlusion technique, as previously described (13). Briefly, male Sprague-Dawley rats weighing 250–300 g were anesthetized with 4% isoflurane in 70% N<sub>2</sub>O/30% O<sub>2</sub> using a mask. The neck was incised in the midline, the right external carotid artery (ECA) was carefully exposed and dissected, and a 19-mm-long 3–0 monofilament nylon suture was inserted from the ECA into the right internal carotid artery to occlude right middle cerebral artery at its origin. After 90 min, the suture was removed to allow reperfusion, the ECA was ligated, and the wound was closed. Sham-operated rats underwent an identical procedure, except that the suture was not inserted. Rectal temperature was maintained at  $37.0 \pm 0.5^\circ\text{C}$  using a heating pad and heating lamp. Regional cerebral blood flow was measured by laser-Doppler flowmetry (Moor Instruments) with the probe positioned over the left hemisphere, 1.5 mm posterior and 3.5 mm lateral to the bregma. After reperfusion for various periods, rats were anesthetized and perfused through the heart with 4% paraformaldehyde in PBS (pH 7.4). All animal experiments were carried out in accordance with National Institutes of Health guidelines and with the approval of the Institutional Animal Care and Use Committee.

### Intracerebroventricular administration of rapamycin

Rats were implanted with an osmotic minipump to the left lateral ventricle 6 h after middle cerebral artery occlusion (MCAO). For neurologic behavioral tests and lesion volume measurement, each rat was intracerebroventricularly infused with 0.5  $\mu\text{l/h}$  of either rapamycin (1  $\mu\text{M}$ ; Calbiochem, La Jolla, CA) or vehicle (artificial cerebrospinal fluid) for 7 d and then sacrificed 28 d after MCAO. For studying neuroinflammatory response, rats were administered either rapamycin or vehicle for 3 d and sacrificed 3 d after treatment.

### Lesion volume measurement

Rats were sacrificed 4 wk after MCAO. Coronal sections (100  $\mu\text{m}$ ; 400  $\mu\text{m}$  apart; 12–16 per rat, 7 rats per group) were stained with crystal violet. Lesion area was measured by a blinded observer, as described previously (14). Lesion volumes were expressed as a percentage of the volume of the structures in the control hemispheres.

### Neurobehavioral testing

Rats underwent neurobehavioral tests to evaluate functional outcome. The neurobehavioral tests, including beam balance test, limb placing test, and elevated body swing test, were performed according to our previous publications (15). Animals were trained prior to surgery, and deficits were assessed 1, 3, 7, 14, and 28 d thereafter. The observer was blinded to the experimental condition.

### Isolation of immune cells from brains

Isolation of brain immune cells was performed following a well-established method (16) with a few modifications at day 3 postischemia. Briefly, rat cerebral hemispheres were cut into  $\sim 1\text{-mm}^3$  pieces before digestion with digestion buffer for 45 min at  $37^\circ\text{C}$ . Digestion buffer consists of RPMI 1640 medium supplemented with 10% FBS, 1 mg/ml collagenase type IV (Sigma-Aldrich), 50  $\mu\text{g/ml}$  DNase I (Sigma-Aldrich), and 5 mM CaCl<sub>2</sub> (Fisher Scientific). Digested tissues were then gently pressed through 40- $\mu\text{m}$  cell strainers to prepare homogenized tissue suspension. Tissue suspension was then mixed with 4 vol of 30% Percoll (GE Healthcare). The mixture was loaded onto 2 ml 37% Percoll, which was above 2 ml 70% Percoll, followed by centrifugation at  $500 \times g$  for 20 min. Cells in the interface between 37% Percoll and 70% Percoll were collected, washed with PBS, and resuspended in PBS for further use.

### Flow cytometry analysis and cell sorting

For immune cell staining, the following anti-rat Abs were used: Alexa Fluor 647 anti-TCR $\alpha\beta$  (R73), FITC anti-TCR $\gamma\delta$  (V65), allophycocyanin-Cy7 anti-CD4 (W3/25), PE anti-CD8 (G28), PE anti-CD25 (OX-39), PE/Cy7 anti-CD45 (OX-1), PE anti-CD11b/c (OX-42), and FITC anti-RT1B (MHC-II, OX-6) (BioLegend); Alexa Fluor 647 anti-CD163 (ED2; AbD Serotec); biotinylated anti-granulocyte (RP-1; BD Pharmingen); and biotinylated or PE anti-CD3 (eBioG4.18; eBioscience). Stained cells were analyzed on a BD LSR-II flow cytometer. Dead cells and debris were excluded by staining with propidium iodide (eBioscience). For Treg detection, Alexa Fluor 488 anti-mouse/rat/human Foxp3 (150D) was purchased from BioLegend. For cell sorting, stained cells were sorted on a BD

InFlux Cell Sorter. For intracellular staining, cells were stained with Abs against surface Ags, followed by fixation, permeabilization, and staining with PE-Cy7 anti-IL-17A (eBio17B7; eBioscience), according to BD intracellular cytokine-staining manual.

### In vitro cell culture

On day 3 after ischemia/reperfusion (I/R), anti-granulocyte<sup>−</sup>CD11b/c<sup>+</sup> myeloid cells (mainly macrophages and microglia) were sorted from vehicle-treated ischemic brain hemispheres by flow cytometry. TCR $\alpha\beta$ <sup>+</sup>CD4<sup>+</sup>CD25<sup>high</sup> Treg-enriched cells were sorted from either vehicle-treated or rapamycin-treated ischemic brain hemispheres by flow cytometry. Treg-enriched cells from 2–3 ischemic brains of each group were pooled. A total of  $1 \times 10^4$  myeloid cells and  $1 \times 10^4$  Treg-enriched cells was cocultured in 96-well V-bottom microplates at  $37^\circ\text{C}$  in RPMI 1640 medium supplemented with 10% FBS, 2 mM L-glutamine, 100 U/ml penicillin, and 100  $\mu\text{g/ml}$  streptomycin. After 24-h coculture, cells were centrifuged at  $1000 \times g$  for 5 min and were incubated in PBS containing 1 mM EDTA and biotinylated anti-CD3 mAb for 15 min on ice. CD3<sup>+</sup> cells (Tregs) were depleted with Dynabeads biotin binder (Invitrogen) following the manufacturer's protocol. Unbound cells were collected and subject to quantitative RT-PCR (Q-RT-PCR). To check the efficiency of Treg depletion, unbound cells were incubated with FITC anti-CD5 mAb (HIS47; eBioscience) and subject to flow cytometry analysis.

To explore the direct effect of rapamycin on myeloid cells, anti-granulocyte<sup>−</sup>CD11b/c<sup>+</sup> myeloid cells were isolated from vehicle-treated ischemic brain hemispheres, as described above, on day 3 after I/R. Cell density was adjusted to  $1 \times 10^6/\text{ml}$  in supplemented RPMI 1640. Fifty microliters of cell suspension was added into each well of a 96-well microplate, and rapamycin was added at a final concentration of 10 nM. Cells were cultured at  $37^\circ\text{C}$  for 24 h before collection for RNA extraction and Q-RT-PCR.

### $\gamma\delta$ T cell migration assay

On day 3 after I/R, spleens from vehicle-treated rats were isolated, and single splenocyte suspension was prepared by mechanical dissociation in 40- $\mu\text{m}$  cell strainers. RBCs were lysed with BD RBC lysis buffer. Splenocytes were incubated with FITC anti-TCR $\gamma\delta$  Ab for 15 min on ice. TCR $\gamma\delta$ <sup>+</sup> cells were sorted by flow cytometry. CD45<sup>high</sup>CD11b/c<sup>+</sup> macrophages and CD45<sup>low</sup>CD11b/c<sup>+</sup> microglia were sorted from vehicle-treated and rapamycin-treated ischemic brain hemispheres by flow cytometry, respectively. All cells were resuspended in supplemented RPMI 1640. A total of  $2 \times 10^5$  macrophages or microglia was seeded into each well of a 96-well Transwell plate (Corning). A total of  $1.25 \times 10^4$   $\gamma\delta$  T cells was seeded into each well of the insert. The cells were cultured at  $37^\circ\text{C}$  for 18 h. All cells in the lower wells (not the insert wells) were then incubated in 1 mM EDTA-PBS for 10 min and collected. Cells were incubated with PE anti-CD3 Ab for 15 min on ice. The number of CD3<sup>+</sup> cells was enumerated by flow cytometry.

### Depletion of Tregs in vivo

To deplete Tregs in vivo, anti-rat CD25 mAb (OX-39; AbD Serotec) was used according to previous literature with modifications (17, 18). Briefly, 2.5 mg Ab in PBS was i.p. injected into each rat once per day for 2 d prior to I/R. Peripheral blood was collected through tail vein at indicated time points to determine the efficiency of Treg depletion by flow cytometry analysis. Rats receiving PBS were used as vehicle control.

### Q-RT-PCR

Total RNAs were reversely transcribed to cDNAs using SuperScript III First-Strand Synthesis System (Invitrogen), according to the manufacturer's instructions. Q-RT-PCR was performed using Fast SYBR Green Master Mix (Invitrogen) on a 7300 Real-Time PCR System (Invitrogen). Data were analyzed with 7300 system software. Primer sequences for each gene were shown in Table I.

### Western blot

Western blot was performed using the protocol as previously described (19). The primary Abs were anti-phospho-4EBP1 (Thr<sup>37/46</sup>), anti-4EBP1 (Cell Signaling), and anti-actin (Santa Cruz Biotechnology). Membranes were developed with SuperSignal West Pico Chemiluminescent Substrate (Thermo Scientific), and the OD was analyzed using a Biospectrum 500 imaging system (Ultra-Violet Products).

### Statistical analyses

Quantitative data were expressed as mean  $\pm$  SEM from the indicated number of experiments. Behavioral data were analyzed by two-way

ANOVA with repeated measures, followed by post hoc multiple comparison tests (Fisher protected least significant difference or Student paired *t* test with the Bonferroni correction). Lesion volume data were analyzed by one-way ANOVA, followed by Fisher protected least significant difference post hoc tests. For quantifying immune cellularity and cytokine expression, Student *t* test or one-way ANOVA was used for comparison of mean between the groups. The *p* values <0.05 were considered significant.

## Results

### Rapamycin reduces lesion volume and improves motor deficits after MCAO

To assess the role of rapamycin after focal ischemia, rapamycin or vehicle was administered beginning 6 h, which corresponds more closely to the clinical setting, after MCAO for consecutive 7 d, and rats were euthanized 4 wk after MCAO to measure lesion volume (Fig. 1A). As shown in Fig. 1B and 1C, lesion volume was significantly decreased in the rapamycin- compared with vehicle-treated group. Next, we asked whether blocking mTOR signaling could improve the neurologic deficits after MCAO. As shown in Fig. 1D, there was a significant difference in the motor performance as observed in beam balance test, limb placing test, and elevated body swing test between rapamycin- and vehicle-treated groups, consistent with the effect of rapamycin in functional outcome in rats after I/R.

### Rapamycin reduces $\gamma\delta$ T cell and granulocyte infiltration

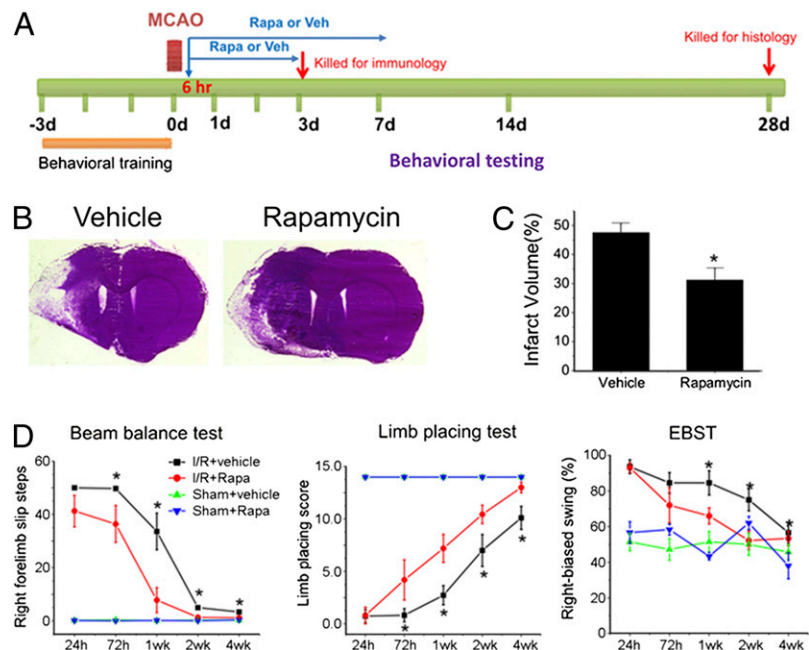
Expression of proinflammatory cytokines and chemokines such as TNF- $\alpha$ , IL-1 $\beta$ , CCL2, and CCL3 is induced as early as 1–2 h after ischemia and is increased for up to 2–5 d (20–25). Importantly, the temporal profile of chemokines such as CCL2 and CCL3 is in line with that of leukocyte accumulation in the ischemic brain parenchyma (26). Leukocyte accumulation is the character of inflammation. Previous studies have indicated that leukocyte accumulation, including T cells, B cells, granulocytes, and monocytes, starts on day 1 and peaks on day 3 after onset of ischemia (16, 27). Thus, postischemic neuroinflammation appears to culminate at day 3 after I/R. So we chose this time point to study the neuroinflammation, hoping to observe significant changes and easily isolate recruited leukocytes. To investigate the mechanism by which rapamycin protected from MCAO-induced damage, we first

determined whether rapamycin inhibited inflammatory cell infiltration in the ischemic brain. Total immune cells recovered from rapamycin-treated brains 3 d after ischemia were significantly less than those from vehicle-treated brain (Fig. 2A). We then investigated distinct leukocyte populations. Leukocytes were carefully gated based on CD45 expression and their specific surface markers (Supplemental Fig. 1A). In the ipsilateral (ischemic) hemispheres, there was no significant difference in  $\alpha\beta$  T cell number between rapamycin- and vehicle-treated groups (Fig. 2B), although a trend of decrease in CD4<sup>+</sup> T cells occurred. In contrast, infiltration of  $\gamma\delta$  T cells and granulocytes in the ipsilateral hemisphere was profoundly inhibited in rapamycin-treated rats compared with vehicle-treated rats (Fig. 2C, 2E). Previous study has shown the pivotal role of  $\gamma\delta$  T cell-derived IL-17 in the progression of postischemic neuroinflammation in mice (16). Thus, we determined IL-17A expression in infiltrated  $\gamma\delta$  T cells to check whether rapamycin could influence IL-17A expression. To our surprise, neither IL-17A protein nor IL-17A mRNA was significantly elevated in infiltrated  $\gamma\delta$  T cells, and rapamycin had no significant effect on IL-17A expression in  $\gamma\delta$  T cells (Fig. 2D, Supplemental Fig. 1B). These data suggest that, unlike mouse MCAO model, IL-17 might not be an important factor for  $\gamma\delta$  T cell-induced neuroinflammation in rat ischemia.

### Rapamycin inhibits production of proinflammatory cytokines and chemokines by macrophages and microglia

The reduction of immune cells in the ipsilateral hemisphere suggests that recruitment of  $\gamma\delta$  T cells and granulocytes by postischemic neuroinflammation is restrained by rapamycin treatment. Macrophages and microglia play critical roles in the initiation of postischemic neuroinflammation, including recruitment of blood leukocytes. Therefore, we tested macrophage/microglia-mediated inflammation by detecting production of cytokines and chemokines in these cells. The amount of CD45<sup>high</sup>CD11b<sup>+</sup> macrophages and CD45<sup>low</sup>CD11b<sup>+</sup> microglia was significantly increased in ipsilateral hemispheres in comparison with the contralateral side, but rapamycin treatment did not alter their number, suggesting rapamycin has no effect on the accumulation of macrophages and microglia after stroke (Fig. 3A). Q-RT-PCR with specific primers (Table I) revealed that I/R robustly induced expression of in-

**FIGURE 1.** Rapamycin treatment reduced lesion volume and improved motor deficits after MCAO. **(A)** The scheme of experimental design. **(B)** Crystal violet-stained coronal brain sections from rapamycin- and vehicle-treated ischemic rats. **(C)** Volume loss in vehicle- and rapamycin-treated rats (*n* = 7 per group). **(D)** Neurobehavioral tests (sham group: *n* = 6–7; MCAO group: *n* = 10–11). *Left*, Beam-walking test scores, expressed as the mean numbers of forelimb slip steps when traversing an elevated narrow beam; *middle*, limb-placing test scores, expressed as a score derived from the number of correct limb placements; *right*, elevated body swing test scores, expressed as a percentage of turns to the contralesional (impaired) side. \**p* < 0.05 compared with vehicle-treated rats. Rapa, rapamycin; Veh, vehicle.





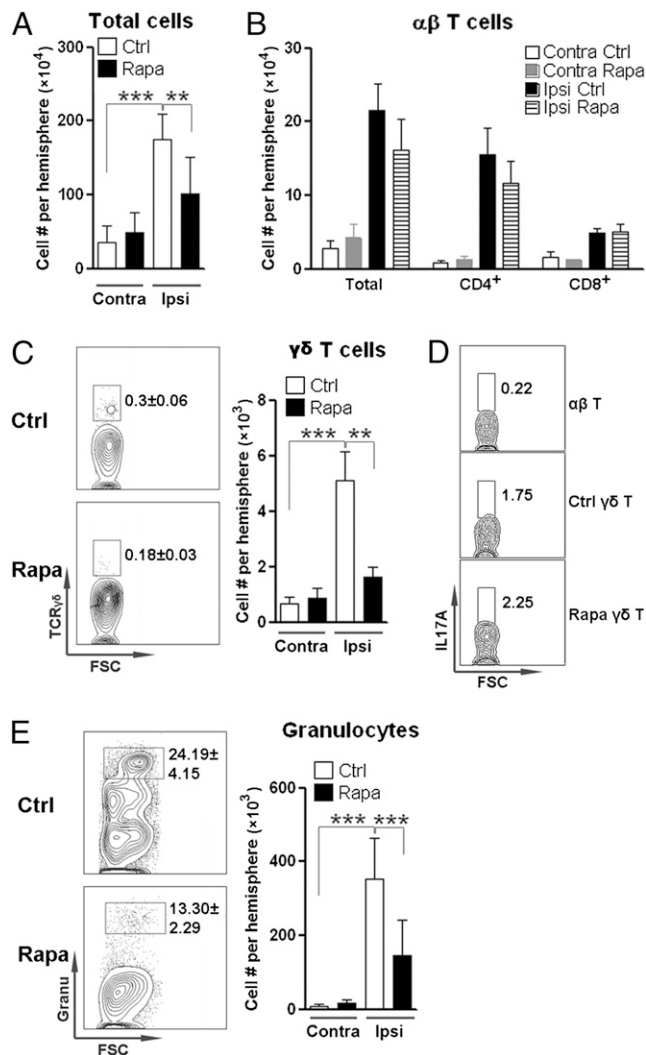


**FIGURE 2.** Rapamycin treatment reduced inflammatory cell infiltration after MCAO. (A) The number of total immune cells recovered from ischemic brains. (B)  $\alpha\beta$  T cell number in ischemic brains. (C)  $\gamma\delta$  T cell number in ischemic brains. Left, Representative contour plots of brain  $\gamma\delta$  T cells. Right, Statistical analysis of  $\gamma\delta$  T cell infiltrates. (D) Flow cytometry analysis of IL-17A expression in infiltrated T cells.  $\alpha\beta$  T,  $\alpha\beta$  T cells; Ctrl  $\gamma\delta$  T,  $\gamma\delta$  T cells in brains of vehicle-treated rats; Rapa  $\gamma\delta$  T,  $\gamma\delta$  T cells in brains of rapamycin-treated rats. This is a representative of three independent experiments. (E) Granulocyte number in ischemic brains. Left, Representative contour plots of brain granulocytes. Right, Statistical analysis of granulocyte infiltrates. Numbers in the plots are the frequencies of each population in total recovered immune cells.  $n = 8$  rats per group.  $**p < 0.01$ ,  $***p < 0.001$ . Contra, contralateral side; Ctrl, vehicle control; Ipsi, ipsilateral side; Rapa, rapamycin treated.

flammatory cytokines and chemokines in macrophages and microglia in ischemic hemispheres (Supplemental Fig. 2A). Note that induction of IL-23a (p19) and IL-12b (p40) was not as profound as induction of other cytokines (Supplemental Fig. 2A), suggesting that expression of IL-23 might be relatively low in our model. This could explain why we did not observe significant IL-17 expression in  $\gamma\delta$  T cells. Compared with vehicle treatment, rapamycin treatment inhibited expression of TNF- $\alpha$ , IL-1 $\beta$ , IL-6, inducible NO synthase (iNOS), and IL-12b (p40) in macrophages, whereas IL-23a (p19) expression was not affected (Fig. 3B), suggesting that rapamycin downregulates proinflammatory activity of macrophages. In microglia, only IL-1 $\beta$  expression was significantly downregulated by rapamycin treatment, although there was a trend of decrease in TNF- $\alpha$  and iNOS expression

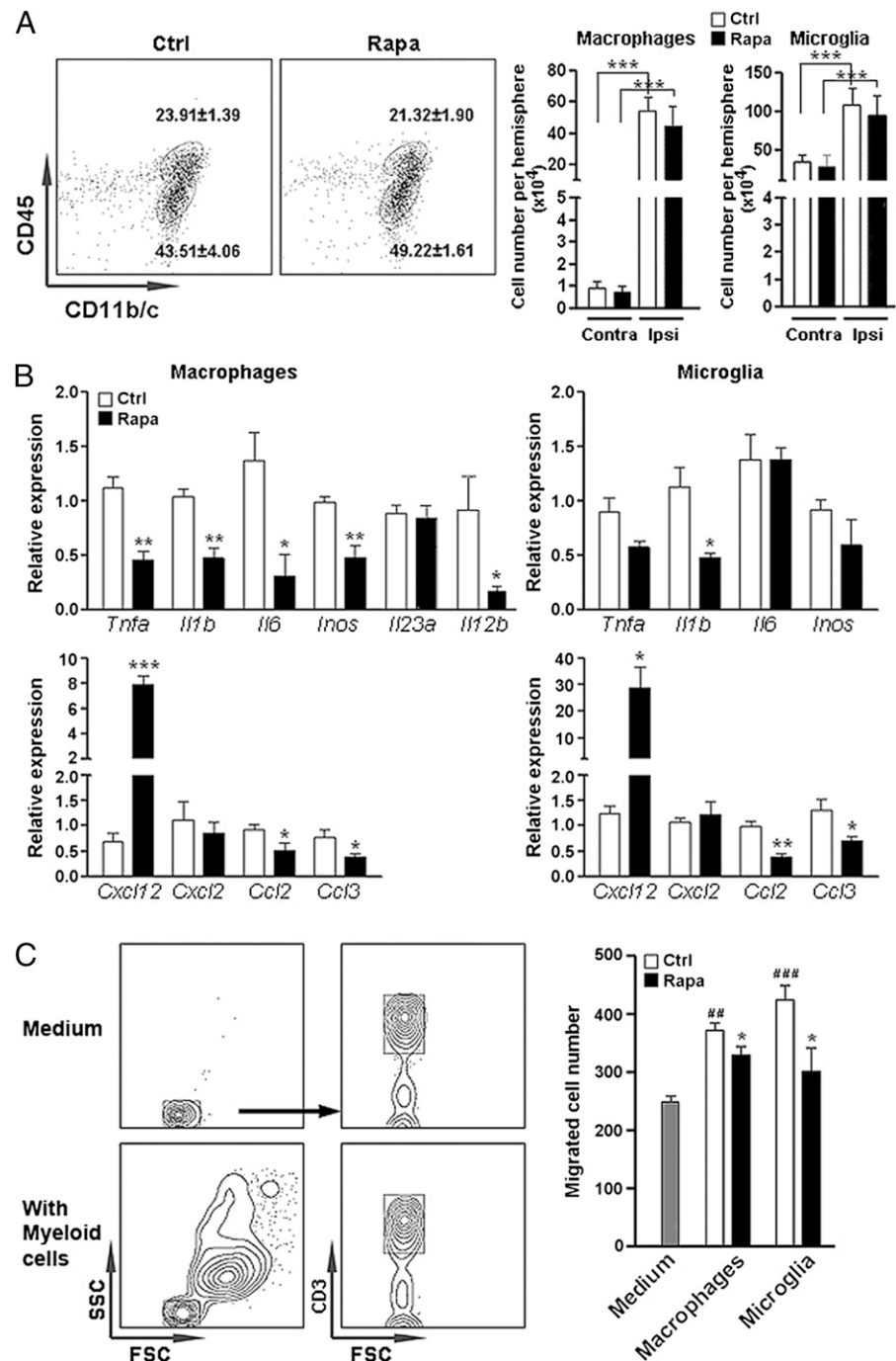
Table I. Primer sequences for Q-RT-PCR

Genes	Primers (Forward and Reverse)
<i>Il10</i>	5'-TAAAAGCAAGGCAGTGGAGC-3' 5'-GATGCCGGTGGTTCAATTT-3'
<i>Tgfb1</i>	5'-GTCAACTGTGGAGCAACACG-3' 5'-TTCCGTCTCCTTGGTTCAGC-3'
<i>Ebi3</i>	5'-TTCTAGCCTTTGTGGCGGAA-3' 5'-AGCGAAGTCGGTACTTGAGAG-3'
<i>Tnfa</i>	5'-TCGGTCCCAACAAGGAGGAG-3' 5'-GGGCTTGTCACTCGAGTTTGTG-3'
<i>Il1b</i>	5'-TGCTGACCCATGTGAGCTG-3' 5'-GCCACAGGGATTTTGTCTGTT-3'
<i>Il6</i>	5'-ACTTCACAAGTCGGAGGCTT-3' 5'-TTCTGACAGTGCATCATCGCT-3'
<i>Inos</i>	5'-TTCTCAGGCTTGGTCTTGT-3' 5'-GGCAAGCCATGTCTGTGACTT-3'
<i>Il23a</i>	5'-CTCTGTAATGCGCTTAGTC-3' 5'-GCTTTTGTACAGGTCCGTAT-3'
<i>Il12b</i>	5'-TCCAGACACATCAGACCAAGCA-3' 5'-AGTGGAGACACCAGCAAAACC-3'
<i>Ikzf2</i>	5'-ATAACGTCAAGTGACAATGAGCTT-3' 5'-CTTCATCACTCTGCATTTCCAGC-3'
<i>Nrp1</i>	5'-AGCTACTGGCTGGGAAGTA-3' 5'-CTGGTCATCGTCACACTCG-3'
<i>Fgf2</i>	5'-CCGGTACCTGGCTATGAAGG-3' 5'-TTCCGTGACCGGTAAGTGT-3'
<i>Cxcl12</i>	5'-CTGCCGATTCTTTTGAGAGCCA-3' 5'-GGGCTGTTGTGCTTACTTGT-3'
<i>Cxcl2</i>	5'-ACATCCAGAGCTTGACGGTG-3' 5'-CAGGTCAGTTAGCCTTGCCCT-3'
<i>Ccl2</i>	5'-TAGCATCCAGCTGCTGTCTC-3' 5'-CAGCCGACTCATTTGGGATCA-3'
<i>Ccl3</i>	5'-CTCAGCACCATGAAGGTCTCC-3' 5'-CGTCCATAGGAGAAGCAGCAG-3'
<i>Gapdh</i>	5'-GATGGTGAAGGTCTGGTGA-3' 5'-TGAAGTTCGGTGGGTAGAG-3'

(Fig. 3B). To our surprise, rapamycin strongly increased CXCL2 mRNA level in macrophages and microglia. In addition, rapamycin significantly reduced CCL2 and CCL3 level in macrophages and microglia (Fig. 3B). The reduction of CCL2 and CCL3 levels could be a reason of reduced leukocyte infiltration in the ischemic brains. To test our hypothesis that rapamycin weakens macrophage/microglia-induced chemoattraction of  $\gamma\delta$  T cells, we performed in vitro migration assay by culturing splenic  $\gamma\delta$  T cells with postischemic brain macrophages or microglia in the Transwell plates. Both macrophages and microglia effectively induced migration of  $\gamma\delta$  T cells 18 h after culture. Compared with control groups, macrophages and microglia isolated from rapamycin-treated brains induced less  $\gamma\delta$  T cell migration, suggesting their ability to recruit  $\gamma\delta$  T cells is indeed weakened (Fig. 3C).

The changes in cytokine and chemokine expression could be due to direct or indirect effect of rapamycin on macrophages and microglia. To clarify this, we isolated macrophages and microglia from ischemic rat brains without rapamycin injection. These cells were cultured in vitro in the presence or absence of rapamycin for 24 h, and mRNA levels of cytokines and chemokines were tested by Q-RT-PCR. Rapamycin directly enhanced expression of IL-1 $\beta$ , iNOS, CCL3, and IL-23a, but did not affect expression of TNF- $\alpha$ , IL-6, CXCL2, and IL-12b in macrophages (Supplemental Fig. 2B). In microglia, expression of IL-1 $\beta$  and iNOS was also promoted by rapamycin (Supplemental Fig. 2B). Our data are generally consistent with previous publications that demonstrated that rapamycin enhances proinflammatory activity of macrophages (28, 29). Thus, in vivo decrease of proinflammatory mediators in macrophages and microglia is unlikely due to the direct effect of rapamycin. It is more likely that rapamycin acts on other cell types first, and, in turn, those affected cell types induce less inflammatory response of macrophages and microglia. Interestingly, rapamycin

**FIGURE 3.** Rapamycin treatment inhibited proinflammatory activity of macrophages and microglia. **(A)** Macrophages and microglia in ischemic brains. *Left*, Representative dot plots of flow cytometry analysis showing brain macrophages and microglia. Total isolated cells were gated according to CD45 and CD11b/c expression. Numbers in the plots are the frequencies of each population in total recovered immune cells. *Right*, The number of macrophages and microglia in ischemic brains with or without rapamycin treatment, respectively. \*\*\* $p < 0.001$ . **(B)** Q-RT-PCR for mRNA levels of cytokines and chemokines in brain macrophages and microglia after MCAO.  $n = 6$  rats per group. \* $p < 0.05$ , \*\* $p < 0.01$ , \*\*\* $p < 0.001$ . **(C)** In vitro migration of  $\gamma\delta$  T cells induced by macrophages and microglia. *Left*, Representative contour plots of flow cytometry analysis showing the gating strategy.  $\gamma\delta$  T cells were first gated based on forward and side light scatter, then were further gated by CD3 expression. *Right*, The number of  $\gamma\delta$  T cells migrating to the lower wells. Medium, random migration of  $\gamma\delta$  T cells without macrophages or microglia in the lower wells. Macrophages, migration of  $\gamma\delta$  T cells induced by macrophages. Microglia, migration of  $\gamma\delta$  T cells induced by microglia.  $n = 3$  per group. ## $p < 0.01$  compared with medium only, ### $p < 0.001$  compared with medium only, \* $p < 0.05$  compared with migration induced by macrophages or microglia isolated from vehicle-treated rats. Contra, contralateral side; Ctrl, vehicle control; Ipsi, ipsilateral side; Rapa, rapamycin-treated rats.



mycin directly inhibited CCL2 expression in both macrophages and microglia (Supplemental Fig. 2B), which is consistent with the in vivo data. CCL2 has been shown to be critical for  $\gamma\delta$  T cell recruitment in other disorders (30, 31). Hence, rapamycin might directly inhibit CCL2 production in macrophages and microglia, so as to reduce  $\gamma\delta$  T cell accumulation in ischemic brains.

The expression of anti-inflammatory TGF- $\beta$ 1 and IL-10 was not altered in macrophages and microglia (Supplemental Fig. 3A, 3B). Expression of fibroblast growth factor-2 was upregulated in microglia from rapamycin-treated brains, suggesting microglia might promote brain recovery.

#### Rapamycin treatment favors brain macrophage polarization toward M2 type

Polarization of macrophages between M1 and M2 type is associated with pro- and anti-inflammatory activity, respectively.

Above data suggest that polarization of macrophages and microglia might be changed after rapamycin treatment. Our flow cytometry analysis showed that four subpopulations of macrophages—RT1B<sup>+</sup>CD163<sup>+</sup>, RT1B<sup>+</sup>CD163<sup>+</sup>, RT1B<sup>+</sup>CD163<sup>+</sup>, and RT1B<sup>+</sup>CD163<sup>+</sup>—were present in contralateral hemispheres (Supplemental Fig. 4). According to published M1 and M2 phenotypes (32, 33), we designated them M0, M1, M1/2, and M2, respectively. However, only very few microglia in contralateral hemispheres expressed RT1B or CD163 (Supplemental Fig. 4). In ipsilateral hemispheres, rapamycin treatment increased the frequency and number of M2 macrophages, compared with vehicle control (Fig. 4A, 4B), suggesting rapamycin treatment favors M2 polarization of macrophages. To our surprise, microglia barely expressed RT1B and CD163 in both contralateral and ipsilateral hemispheres (Fig. 4C, Supplemental Fig. 4), suggesting that

these surface markers are not suitable for distinguishing microglial polarization.

#### Rapamycin enhances anti-inflammatory activity of Tregs

It has been shown that rapamycin enriched the population of Tregs (34–36). Tregs are able to protect ischemic brain damage (37). So we asked whether rapamycin could alter Treg number and/or activity in ischemic brains. Treg number in rapamycin-treated brains was comparable to that in vehicle-treated brains. However, the proportion of Tregs in total recovered immune cells was significantly increased (Fig. 5A). Tregs in rapamycin-treated brains expressed higher Foxp3 and CD25 (Fig. 5B), suggesting they have higher regulatory activity than Tregs in the vehicle control brains. To determine the anti-inflammatory activity of Tregs, we sorted  $\text{TCR}\alpha\beta^+\text{CD4}^+\text{CD25}^{\text{high}}$  Treg-enriched cells for Q-RT-PCR (Table I). mRNA levels of IL-10 in Tregs were not significantly changed, whereas mRNA levels of TGF- $\beta$ 1 and Ebi3 were elevated in Tregs in rapamycin-treated brains (Fig. 5C). Thus, rapamycin treatment enhanced Treg anti-inflammatory activity. Q-RT-PCR revealed that infiltrated Tregs expressed similar levels of helios and neuropilin-1 as those in splenic counterparts (Fig. 5D). Splenic Tregs contain mainly natural Tregs (38). Hence, infiltrated Tregs are mainly natural Tregs as well. This result is consistent with our expectation based on the temporal process of immune response, because adaptive immune reaction has not fully engaged on day 3 after Ag exposure.

#### Tregs in rapamycin-treated brains inhibit proinflammatory activity of macrophages/microglia

Then we tested whether Tregs in rapamycin-treated brains more potently inhibit macrophage/microglia-mediated inflammation. Because rapamycin treatment induced a similar cytokine/chemokine expression change in macrophages and microglia (Fig. 3B), we used macrophage/microglia mixture for the study. Ischemic macrophages/microglia were cocultured with Tregs isolated from ischemic brains. Tregs, which are  $\text{CD5}^+$ , were then effectively depleted with magnetic beads (Fig. 6A). Tregs from vehicle-treated brains moderately inhibited cytokine/chemokine expression, except for TNF- $\alpha$  and CCL2, whereas Tregs from rapamycin-treated brains more robustly inhibited almost all cytokines/chemokines in comparison with Tregs from vehicle-treated brains (Fig. 6B). To confirm that rapamycin inhibited mTOR signaling, brain immune cells were isolated to measure mTOR complex 1 activity by Western blot. Ischemic injury significantly upregulated 4EBP1 and phosphorylated 4EBP1. Rapamycin treatment did not alter 4EBP1 protein levels but significantly reduced 4EBP1 phosphorylation (Fig. 6C). Thus, rapamycin downregulated mTOR complex 1 signaling in infiltrating leukocytes.

#### Depletion of Tregs partially elevates inflammatory response of macrophages/microglia in rapamycin-treated ischemic brains

To further explore whether Tregs are critical for rapamycin-induced alleviation of neuroinflammatory response in macrophages/microglia, i.p. injection of anti-CD25 Ab was applied to deplete peripheral Tregs before MCAO was performed (Fig. 7A). Peripheral blood was drawn to determine the efficiency of Treg depletion. Three days and 5 d after the initial Ab injection, >50 and 60% of  $\text{CD4}^+\text{Foxp3}^+$  Tregs in the blood were depleted, respectively (Fig. 7B). MCAO and rapamycin injection was performed 2 d after the initial Ab injection. On day 3 after MCAO, brain immune cells were evaluated. Consistent with the reduction of peripheral Tregs, infiltrated Tregs in ischemic brains were also

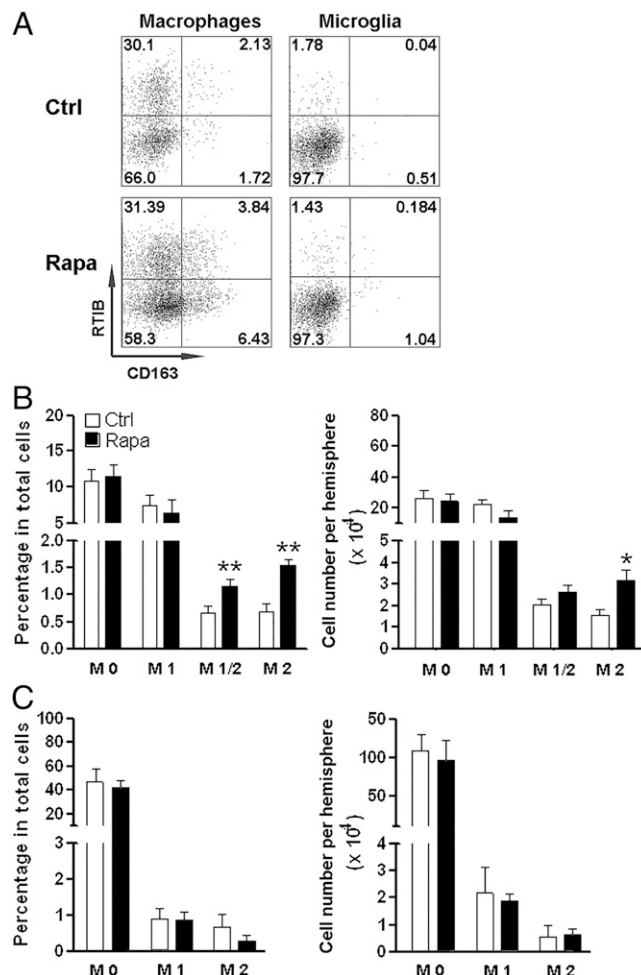


**FIGURE 4.** Rapamycin treatment enhanced brain macrophage polarization into type M2. (A) Representative dot plots of polarization of brain macrophages and microglia. Macrophages and microglia were gated as in Fig. 3A. Then each population was further divided according to MHC-II and CD163 expression. Numbers are the frequency of each population in the parental population. (B) Statistical analysis of frequency (left) and cell number (right) of each macrophage subtype. (C) Statistical analysis of frequency (left) and cell number (right) of each microglia subtype. All data are from ipsilateral hemispheres.  $n = 6\sim 8$  per group. \* $p < 0.05$ , \*\* $p < 0.01$  compared with control group. Ctrl, vehicle control; Rapa, rapamycin treated.

decreased by 60% after Ab treatment (Fig. 7C). In comparison with rats receiving rapamycin and PBS, Treg depletion caused a trend of increase in total immune cell number (Fig. 7D). In comparison with control rats (I/R without additional treatment), the total immune cell number after Treg depletion was relatively lower, but it was not statistically significant (Fig. 7D). Treg depletion induced significant increase of  $\gamma\delta$  T cells and granulocytes in ischemic brains, compared with rats receiving rapamycin and PBS (Fig. 7E). However, their numbers were still less than the amount of  $\gamma\delta$  T cells and granulocytes in ischemic brains of control rats, suggesting Treg depletion only partially increases the infiltration of  $\gamma\delta$  T cells and granulocytes. The numbers of infiltrated  $\alpha\beta$  T cells, macrophages, and microglia were not significantly altered by Treg depletion (Fig. 7E, 7F).

We then tested the cytokine and chemokine production by macrophages/microglia in ischemic brains after Treg depletion. As shown in Fig. 7G, in comparison with administration of rapamycin and PBS, Treg depletion caused significant increases in the mRNA levels of IL-6, iNOS, CCL2, and IL-12b (p40). However, com-



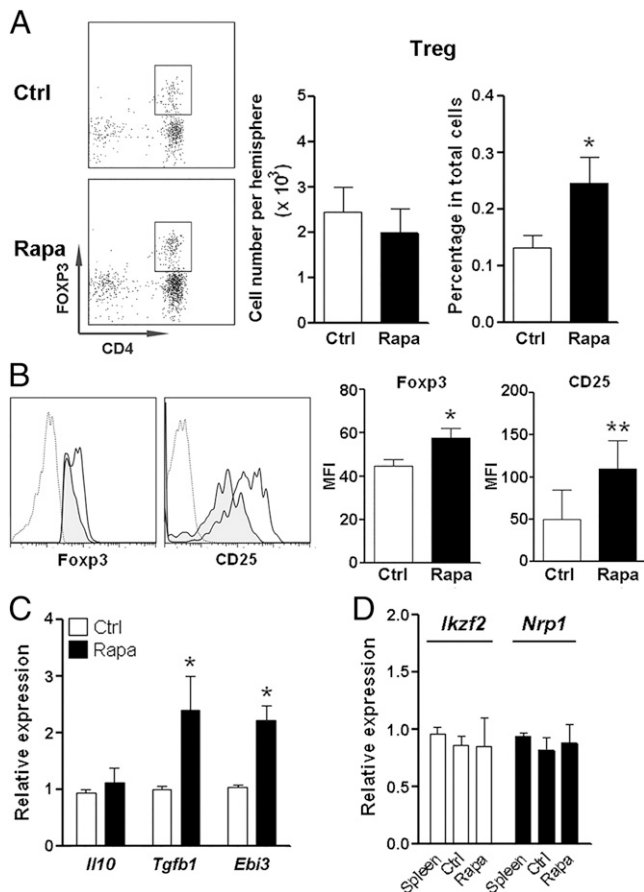


**FIGURE 5.** Rapamycin administration enhanced Treg proportion and activity after MCAO. **(A)** Foxp3<sup>+</sup> Treg number and proportion in ischemic brains. *Left*, Representative dot plots of Foxp3<sup>+</sup> cells gated on CD3<sup>+</sup>CD4<sup>+</sup> T cells in ischemic brains. *Right*, Statistical analysis of Treg number and frequency.  $n = 5$  per group. **(B)** Rapamycin treatment enhanced expression of Foxp3 and CD25 in infiltrating Tregs. *Left*, Representative histograms of Foxp3 and CD25 in Foxp3<sup>+</sup> T cells. Dotted curve, isotype control; shaded curve, vehicle-treated rats; solid curve, rapamycin-treated rats. *Right*, Statistical analysis of the mean fluorescence intensity of Foxp3 and CD25.  $n = 5$  per group. **(C)** Anti-inflammatory cytokine production in Tregs. Data were from ipsilateral hemispheres.  $n = 5$ –6 per group. \* $p < 0.05$ , \*\* $p < 0.01$ . Ctrl, vehicle control; Rapa, rapamycin-treated rats. **(D)** Expression of helios and neuropilin-1 in Tregs detected by Q-RT-PCR.  $n = 3$  per group. Ctrl, Tregs from vehicle control rat brains; Rapa, Tregs from rapamycin-treated rat brains; Spleen, splenic Tregs.

pared with untreated control group, mRNA levels of IL-6 and IL-12b after Treg depletion were still lower. Only iNOS and CCL2 production was relatively close to the control level. There was a trend of increase in the TNF- $\alpha$  mRNA level after Treg depletion, but it was statistically insignificant. Production of IL-1 $\beta$  and CCL3 was almost not changed. Our data suggest Tregs indeed play a role in rapamycin-induced restraint of neuroinflammatory response of macrophages/microglia. However, the effect of Tregs was not as profound as we expected. Some other cellular components might have contributed to the efficacy of rapamycin. Phenotypic polarization of macrophages was not altered after Treg depletion in comparison with vehicle-treated group (Fig. 7H).

## Discussion

The results presented in this work reveal that rapamycin administration 6 h after focal cerebral ischemia significantly reduces lesion volume and improves motor deficits, implying a longer therapeutic window of opportunity for ischemic stroke treatment.

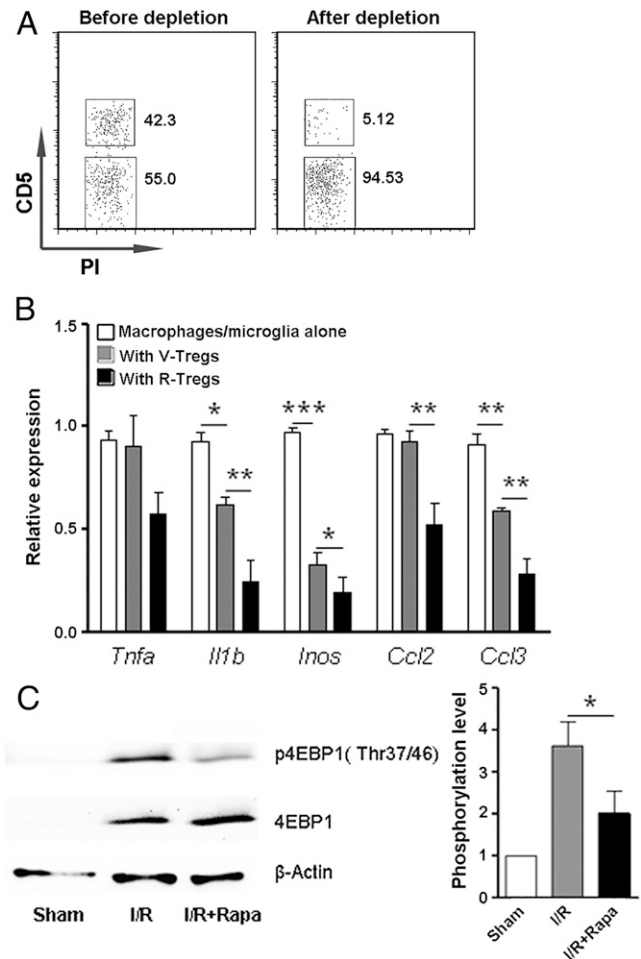


**FIGURE 6.** Tregs in rapamycin-treated rat brains potentially inhibited inflammatory response of macrophages/microglia. **(A)** Magnetic cell sorting effectively depleted Tregs from the coculture. Propidium iodide<sup>+</sup> live cells were detected for expression of CD5. **(B)** Cytokine/Chemokine production in macrophages/microglia after coculture with Tregs.  $n = 5$  per group. **(C)** Phosphorylation of 4EBP1 in immune cells in ischemic brains. This is a representative of three independent experiments.  $n = 4$  per group. \* $p < 0.05$ , \*\* $p < 0.01$ , \*\*\* $p < 0.001$ . Rapa, rapamycin treated rats; R-Tregs, Tregs from rapamycin-treated brains; V-Tregs, Tregs from vehicle-treated brains.

In addition, rapamycin is able to modulate poststroke neuroinflammatory responses by reducing deleterious and enhancing protective actions of immune cells.

Poststroke neuroinflammation plays critical roles in the pathophysiology of ischemic stroke, which is characterized by peripheral leukocyte influx into the cerebral parenchyma, activation of endogenous microglia, and release of proinflammatory mediators (5, 39). These mediators lead to secondary injury of potentially salvageable tissue within the penumbra regions after ischemic stroke. Granulocytes are generally the first leukocyte subtype recruited to the ischemic brain and may potentiate injury by secreting deleterious neuroinflammatory mediators (40). T lymphocytes also influence the ischemic lesion independently of Ag specificity and costimulatory molecules (41), although there are conflicting data (42). The impact of T cell subsets on secondary infarct progression has been disclosed in recent years.  $\gamma\delta$  T cells have pivotal roles in the evolution of brain infarction and accompanying neurologic deficits (16). In contrast, Tregs prevent secondary infarct growth (37). However, their protective role still needs further confirmation because controversies emerge (43, 44).



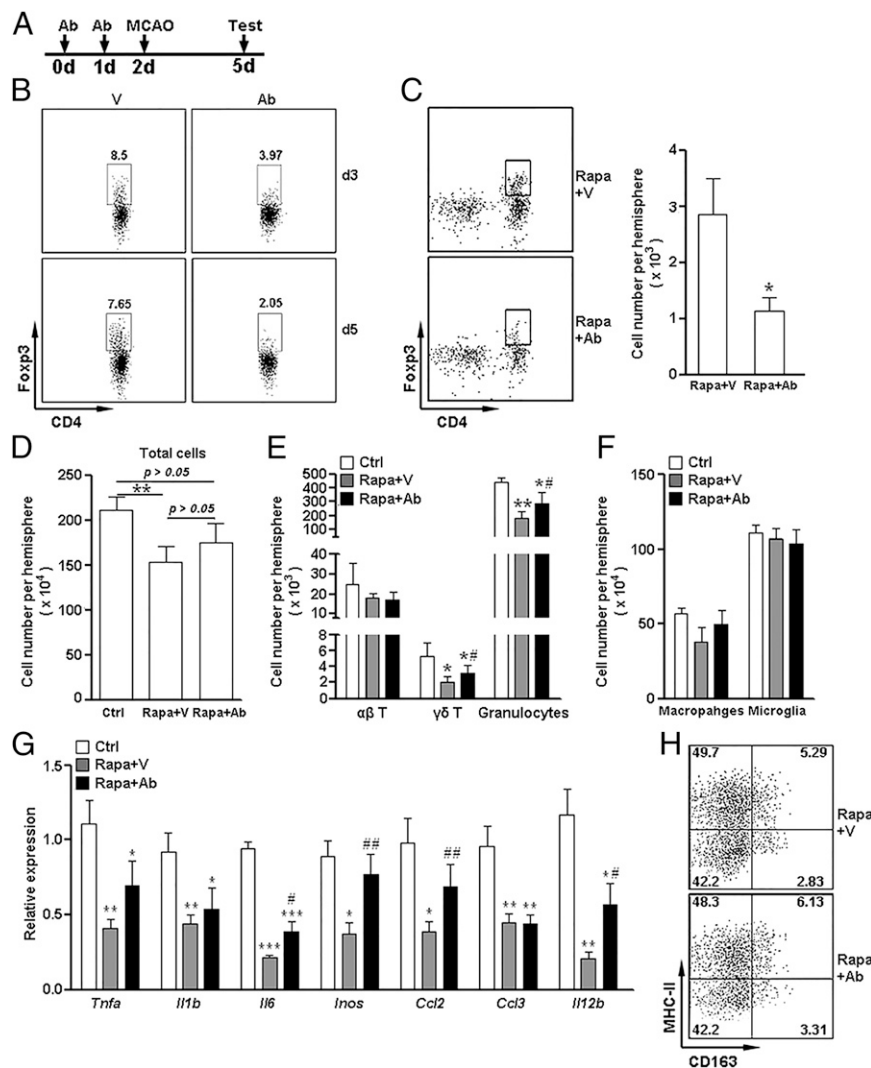


**FIGURE 7.** Depletion of Tregs partially promotes inflammatory response of macrophages/microglia in rapamycin-treated ischemic brains. **(A)** The scheme of experimental design. Anti-CD25 Ab was injected once per day for 2 d before MCAO and rapamycin treatment. On day 5 after the initial injection of Ab, rats were sacrificed for testing neuroinflammation. **(B)** Depletion of CD4<sup>+</sup>Foxp3<sup>+</sup> T cells in the blood on days 3 and 5 after Ab injection. CD3<sup>+</sup>CD4<sup>+</sup> cells were gated for detecting Foxp3<sup>+</sup> cells. The numbers in the plots are the frequencies of Foxp3<sup>+</sup> cells in CD4<sup>+</sup> T cells. This is a representative of two independent experiments. Ab, Ab injection; V, PBS (vehicle) injection. **(C)** Decrease of infiltrated Tregs in ischemic brains after Treg depletion. CD3<sup>+</sup> cells were gated for detecting CD4<sup>+</sup>Foxp3<sup>+</sup> cells. *Left*, Representative dot plot of infiltrated Tregs after MCAO. *Right*, Number of infiltrated Tregs in ipsilateral hemispheres. *n* = 4 per group. \**p* < 0.05. Rapa + Ab, Ab injection before MCAO and rapamycin treatment; Rapa + V, PBS injection before MCAO and rapamycin treatment. **(D–F)** The number of total immune cells (D); αβ T cells, γδ T cells, and granulocytes (E); and macrophages and microglia (F) in the ipsilateral hemispheres. *n* = 4 per group. \**p* < 0.05 compared with control group, \*\**p* < 0.01 compared with control group, #*p* < 0.05 compared with Rapa + V group. Ctrl, control group (MCAO without additional treatment); Rapa + Ab, Ab injection before MCAO and rapamycin treatment; Rapa + V, vehicle injection before MCAO and rapamycin treatment. **(G)** Cytokine and chemokine expression in infiltrated CD11b/c<sup>+</sup> myeloid cells. *n* = 4 per group. \**p* < 0.05 compared with control group, \*\**p* < 0.01 compared with control group, \*\*\**p* < 0.001 compared with control group, #*p* < 0.05 compared with Rapa + V group, ##*p* < 0.01 compared with Rapa + V group. **(H)** Treg depletion did not affect macrophage phenotype. This is a representative of two independent experiments. The number in each quadrant is the frequency of each subpopulation of macrophages.

In our study, administration of rapamycin profoundly reduced the number of γδ T cells in ischemic brains, suggesting rapamycin might protect brains from γδ T cell-mediated damage. However, we could not detect either IL-17 protein or IL-17 mRNA in infiltrated γδ T cells. It might be possible that rat γδ T cells respond differently from their mouse counterparts, using some mediators other than IL-17 to cause the brain damage. It has been shown that γδ T cells also express TNF-α during the development of experimental autoimmune encephalomyelitis (45). The cytokine profile of infiltrated γδ T cells is still unclear and needs further investigation.

Interestingly, Treg number in rapamycin-treated brains was not significantly altered, but the Treg proportion in brain immune cells

was higher. Thus, it is possible that Tregs can function more efficiently to inhibit inflammatory cells in treated brains. TGF-β and IL-10, which can be produced by Tregs, are shown to be neuroprotective (46–48). Our data showed that, although IL-10 level was not enhanced in Tregs, the levels of IL-35 and TGF-β in Tregs were significantly increased by rapamycin. Hence, increased Treg anti-inflammatory activity may contribute to alleviating brain damage. However, it remains unclear whether rapamycin directly or indirectly enhances Treg anti-inflammatory activity in ischemic brains. It has been reported that mTOR signaling negatively regulates Treg commitment, expansion, and function, whereas rapamycin increases Treg number and enhances Treg activity both in vitro and in vivo (49–56). The effect of rapamycin on Tregs is

associated with stabilization of Foxp3 (50, 53), which is the Treg master regulator controlling Treg development and function. Indeed, we found higher Foxp3 level in Tregs in rapamycin-treated brains, suggesting the expression/stabilization of Foxp3 is enhanced by rapamycin treatment. CD25 expression was also higher on Tregs after rapamycin treatment, possibly due to direct binding of Foxp3 to the promoter region of *Il2ra*. The elevated expression of Ebi3, which is the subunit of IL-35, can also be attributed to higher Foxp3 level, because Ebi3 is a downstream target of Foxp3 (57). However, the higher Foxp3 level in rapamycin-treated Tregs does not explain the unchanged IL-10 and increased TGF- $\beta$ , because there is no convincing proof showing Foxp3 directly regulates expression of these cytokines. Thus, rapamycin might regulate their expression independently of direct effect of Foxp3. The higher CD25 expression might reflect higher level of IL-2R on the surface of Tregs in rapamycin-treated brains, thus making these Tregs possess higher affinity for IL-2, which induces more IL-10 expression (58–60). However, rapamycin itself might inhibit IL-10 mRNA and protein in Tregs, as in macrophages (9). Hence, the unchanged IL-10 level might reflect a balance between the effects of IL-2/IL-2R signaling and mTOR inhibition. Researchers have observed rapamycin-induced TGF- $\beta$  production by lymphocytes and infiltrated Tregs in previous studies (61, 62). Hence, rapamycin might directly increase TGF- $\beta$  production in Tregs through unknown molecular mechanisms. In addition, Tregs might also be modulated by an indirect effect of rapamycin. It has been reported that rapamycin-treated endothelial cells and dendritic cells may promote Treg activity in ischemic brains (63, 64). Hence, rapamycin-treated endothelial or dendritic cells could induce Tregs to produce immunosuppressive cytokines to restrain the inflammation. However, further investigations are in demand to test our hypothesis.

Previous studies have documented the proinflammatory (M1) and anti-inflammatory (M2) macrophages in the postischemic brains (65, 66). Modulation of microglia and macrophage polarization toward the beneficial M2 type would restrain neuroinflammation and favor functional recovery (33). Our work indicated that rapamycin treatment phenotypically inhibited M1 polarization in brain macrophages. Correspondingly, proinflammatory cytokine and chemokine production in macrophages was inhibited. However, M2 type-related anti-inflammatory cytokine production was not increased, suggesting the effects of rapamycin on macrophage polarization are more complicated than expected. It is also possible that phenotypical polarization starts earlier than functional polarization, or restraint of M1 cytokine production is prior to elevation of M2 cytokine production. In microglia, both phenotypical and functional polarization were not as significant as in macrophages, suggesting the effects of rapamycin treatment on microglia could be weak or require longer time. Macrophages and microglia showed similar changes in chemokine levels after rapamycin treatment. The profound elevation of CXCL12 was unexpected but could be involved in the migration of neural stem/progenitor cells to the lesion site. Decreased production of other chemokines could explain reduced infiltration of granulocytes and  $\gamma\delta$  T cells. However, inhibited inflammatory response of macrophages and microglia cannot be attributed to the direct effect of rapamycin, because both our data and previous research demonstrated that rapamycin induces macrophages polarization toward the proinflammatory M1 type (30). Thus, the inhibited M1 polarization of macrophages and microglia should be mediated by agents other than rapamycin itself. Interestingly, our data show that the functional change in macrophages/microglia is at least partially due to their interaction with Tregs. Tregs isolated from rapamycin-treated brains more potently inhibited proinflammatory cytokine and chemokine pro-

duction, consistent with their promoted anti-inflammatory activity. So we concluded that, although rapamycin directly induces M1 polarization of macrophages and microglia, it also strongly enhances Treg activity, which in turn restrains the inflammatory response of macrophages and microglia.

To determine whether Treg is a major target of rapamycin, we depleted Tregs with anti-CD25 Ab before stroke and rapamycin injection. Although Treg depletion was successful, it just partially enhanced inflammatory response in rapamycin-treated brains. It appears that Tregs indeed, but limitedly, contributed to rapamycin-induced anti-inflammation effect. Other cell types might also play roles in this process. Note that rapamycin was injected 6 h after I/R, early before the recruitment of peripheral immune cells. We speculated that rapamycin could inhibit the initiation of neuroinflammation when leukocytes are still outside the brain parenchyma. Both damaged/stressed neurons and reactive astrocytes quickly initiate postischemic inflammation, through producing proinflammatory mediators and educating microglia (42, 67, 68). Rapamycin protects neurons after stroke (12, 69) and inhibits reactive astrocytes (70, 71), thus probably preventing the onset of acute neuroinflammation. Hence, the neuroinflammation might have been alleviated even before Tregs entered the brain parenchyma. Decrease of neuroinflammation on day 3 after stroke might be the outcome of both restrained initiation and inhibited progression of neuroinflammation. Tregs might be just involved in the progression phase. This could explain why Treg depletion could not completely abolish the effect of rapamycin. However, careful studies, especially on the initiation of neuroinflammation shortly after I/R, will be needed to test our hypothesis in the future.

In our study, we injected rapamycin into the lateral ventricles, hoping that it functions mainly in the ischemic brains. Based on former studies, peripheral administration of rapamycin also shows neuroprotective effect after stroke (10, 69). Rapamycin can cross the blood brain barrier into the brain parenchyma even in the steady state (72). Thus, peripheral administration of rapamycin might inhibit leukocyte activation in the periphery, prevent neuron death, and restrain astrocyte reaction in the brain, exerting similar effects to intracerebroventricular injection. However, peripheral administration might severely interfere with functions of the immune system and other vital organs/tissues, which might not be good for patients.

Taken together, our research suggests intraventricular administration of rapamycin after ischemic stroke restrains proinflammatory activity of macrophages and microglia through Tregs. These studies may have implications for novel therapeutic interventions targeting postischemic neuroinflammation in stroke.

## Acknowledgments

Flow cytometry cell sorting was performed by Xiangli Sun in the Flow Cytometry and Laser Capture Microdissection Core Facility at University of North Texas Health Science Center.

## Disclosures

The authors have no financial conflicts of interest.

## References

- Go, A. S., D. Mozaffarian, V. L. Roger, E. J. Benjamin, J. D. Berry, M. J. Blaha, S. Dai, E. S. Ford, C. S. Fox, S. Franco, et al. 2014. Heart disease and stroke statistics—2014 update: a report from the American Heart Association. *Circulation* 129: e28–e292.
- Brott, T., and J. Bogousslavsky. 2000. Treatment of acute ischemic stroke. *N. Engl. J. Med.* 343: 710–722.
- Wang, Y., Z. Zhang, N. Chow, T. P. Davis, J. H. Griffin, M. Chopp, and B. V. Zlokovic. 2012. An activated protein C analog with reduced anticoagulant activity extends the therapeutic window of tissue plasminogen activator for ischemic stroke in rodents. *Stroke* 43: 2444–2449.

4. Wechsler, L. R., and T. G. Jovin. 2012. Intravenous recombinant tissue-type plasminogen activator in the extended time window and the US Food and Drug Administration: confused about the time. *Stroke* 43: 2517–2519.
5. Jin, R., G. Yang, and G. Li. 2010. Inflammatory mechanisms in ischemic stroke: role of inflammatory cells. *J. Leukoc. Biol.* 87: 779–789.
6. Sughrue, M. E., A. Mehra, E. S. Connolly, Jr., and A. L. D'Ambrosio. 2004. Anti-adhesion molecule strategies as potential neuroprotective agents in cerebral ischemia: a critical review of the literature. *Inflamm. Res.* 53: 497–508.
7. Wiederrecht, G. J., C. J. Sabers, G. J. Brunn, M. M. Martin, F. J. Dumont, and R. T. Abraham. 1995. Mechanism of action of rapamycin: new insights into the regulation of G1-phase progression in eukaryotic cells. *Prog. Cell Cycle Res.* 1: 53–71.
8. Laplante, M., and D. M. Sabatini. 2009. mTOR signaling at a glance. *J. Cell Sci.* 122: 3589–3594.
9. Thomson, A. W., H. R. Turnquist, and G. Raimondi. 2009. Immunoregulatory functions of mTOR inhibition. *Nat. Rev. Immunol.* 9: 324–337.
10. Chauhan, A., U. Sharma, N. R. Jagannathan, K. H. Reeta, and Y. K. Gupta. 2011. Rapamycin protects against middle cerebral artery occlusion induced focal cerebral ischemia in rats. *Behav. Brain Res.* 225: 603–609.
11. Carloni, S., S. Girelli, C. Scopa, G. Buonocore, M. Longini, and W. Balduini. 2010. Activation of autophagy and Akt/CREB signaling play an equivalent role in the neuroprotective effect of rapamycin in neonatal hypoxia-ischemia. *Autophagy* 6: 366–377.
12. Fletcher, L., T. M. Evans, L. T. Watts, D. F. Jimenez, and M. Digicaylioglu. 2013. Rapamycin treatment improves neuron viability in an in vitro model of stroke. *PLoS One* 8: e68281.
13. Jin, K., M. Minami, J. Q. Lan, X. O. Mao, S. Bateur, R. P. Simon, and D. A. Greenberg. 2001. Neurogenesis in dentate subgranular zone and rostral subventricular zone after focal cerebral ischemia in the rat. *Proc. Natl. Acad. Sci. USA* 98: 4710–4715.
14. Swanson, R. A., M. T. Morton, G. Tsao-Wu, R. A. Savalos, C. Davidson, and F. R. Sharp. 1990. A semiautomated method for measuring brain infarct volume. *J. Cereb. Blood Flow Metab.* 10: 290–293.
15. Sun, F., L. Xie, X. Mao, J. Hill, D. A. Greenberg, and K. Jin. 2012. Effect of a contralateral lesion on neurological recovery from stroke in rats. *Restor. Neurol. Neurosci.* 30: 491–495.
16. Shichita, T., Y. Sugiyama, H. Ooboshi, H. Sugimori, R. Nakagawa, I. Takada, T. Iwaki, Y. Okada, M. Iida, D. J. Cua, et al. 2009. Pivotal role of cerebral interleukin-17-producing gamma delta T cells in the delayed phase of ischemic brain injury. *Nat. Med.* 15: 946–950.
17. Ghiringhelli, F., N. Larmonier, E. Schmitt, A. Parcellier, D. Cathelin, C. Garrido, B. Chauffert, E. Solary, B. Bonnotte, and F. Martin. 2004. CD4+CD25+ regulatory T cells suppress tumor immunity but are sensitive to cyclophosphamide which allows immunotherapy of established tumors to be curative. *Eur. J. Immunol.* 34: 336–344.
18. Ghiringhelli, F., P. E. Puig, S. Roux, A. Parcellier, E. Schmitt, E. Solary, G. Kroemer, F. Martin, B. Chauffert, and L. Zitvogel. 2005. Tumor cells convert immature myeloid dendritic cells into TGF-beta-secreting cells inducing CD4+CD25+ regulatory T cell proliferation. *J. Exp. Med.* 202: 919–929.
19. Hill, J. J., K. Jin, X. O. Mao, L. Xie, and D. A. Greenberg. 2012. Intracerebral chondroitinase ABC and heparan sulfate proteoglycan glypican improve outcome from chronic stroke in rats. *Proc. Natl. Acad. Sci. USA* 109: 9155–9160.
20. Wang, X., T. L. Yue, F. C. Barone, R. F. White, R. C. Gagnon, and G. Z. Feuerstein. 1994. Concomitant cortical expression of TNF-alpha and IL-1 beta mRNAs follows early response gene expression in transient focal ischemia. *Mol. Chem. Neuropathol.* 23: 103–114.
21. Liu, T., P. C. McDonnell, P. R. Young, R. F. White, A. L. Siren, J. M. Hallenbeck, F. C. Barone, and G. Z. Feuerstein. 1993. Interleukin-1 beta mRNA expression in ischemic rat cortex. *Stroke* 24: 1746–1750; discussion 1750–1741.
22. Wiessner, C., J. Gehrmann, D. Lindholm, R. Töpper, G. W. Kreutzberg, and K. A. Hossmann. 1993. Expression of transforming growth factor-beta 1 and interleukin-1 beta mRNA in rat brain following transient forebrain ischemia. *Acta Neuropathol.* 86: 439–446.
23. Liu, T., R. K. Clark, P. C. McDonnell, P. R. Young, R. F. White, F. C. Barone, and G. Z. Feuerstein. 1994. Tumor necrosis factor-alpha expression in ischemic neurons. *Stroke* 25: 1481–1488.
24. Wang, X., T. L. Yue, F. C. Barone, and G. Z. Feuerstein. 1995. Monocyte chemoattractant protein-1 messenger RNA expression in rat ischemic cortex. *Stroke* 26: 661–665, discussion 665–666.
25. Kim, J. S., S. C. Gautam, M. Choppe, C. Zaloga, M. L. Jones, P. A. Ward, and K. M. Welch. 1995. Expression of monocyte chemoattractant protein-1 and macrophage inflammatory protein-1 after focal cerebral ischemia in the rat. *J. Neuroimmunol.* 56: 127–134.
26. Pantoni, L., C. Sarti, and D. Inzitari. 1998. Cytokines and cell adhesion molecules in cerebral ischemia: experimental bases and therapeutic perspectives. *Arterioscler. Thromb. Vasc. Biol.* 18: 503–513.
27. Gelderblom, M., F. Leypoldt, K. Steinbach, D. Behrens, C. U. Choe, D. A. Siler, T. V. Arumugam, E. Orthey, C. Gerloff, E. Tolosa, and T. Magnus. 2009. Temporal and spatial dynamics of cerebral immune cell accumulation in stroke. *Stroke* 40: 1849–1857.
28. Baker, A. K., R. Wang, N. Mackman, and J. P. Luyendyk. 2009. Rapamycin enhances LPS induction of tissue factor and tumor necrosis factor-alpha expression in macrophages by reducing IL-10 expression. *Mol. Immunol.* 46: 2249–2255.
29. Mercalli, A., I. Calavita, E. Dugnani, A. Citro, E. Cantarelli, R. Nano, R. Melzi, P. Maffi, A. Secchi, V. Sordi, and L. Piemonti. 2013. Rapamycin unbalances the polarization of human macrophages to M1. *Immunology* 140: 179–190.
30. Penido, C., M. F. Costa, M. C. Souza, K. A. Costa, A. L. Candéa, C. F. Benjamim, and Md. Henriques. 2008. Involvement of CC chemokines in gamma delta T lymphocyte trafficking during allergic inflammation: the role of CCL2/CCR2 pathway. *Int. Immunol.* 20: 129–139.
31. Lança, T., M. F. Costa, N. Gonçalves-Sousa, M. Rei, A. R. Grosso, C. Penido, and B. Silva-Santos. 2013. Protective role of the inflammatory CCR2/CCL2 chemokine pathway through recruitment of type 1 cytotoxic gamma delta T lymphocytes to tumor beds. *J. Immunol.* 190: 6673–6680.
32. Biswas, S. K., and A. Mantovani. 2010. Macrophage plasticity and interaction with lymphocyte subsets: cancer as a paradigm. *Nat. Immunol.* 11: 889–896.
33. Murray, P. J., and T. A. Wynn. 2011. Protective and pathogenic functions of macrophage subsets. *Nat. Rev. Immunol.* 11: 723–737.
34. Wang, X., W. Wang, J. Xu, and Q. Le. 2013. Effect of rapamycin and interleukin-2 on regulatory CD4+CD25+Foxp3+ T cells in mice after allogeneic corneal transplantation. *Transplant. Proc.* 45: 528–537.
35. Wang, Y., G. Camirand, Y. Lin, M. Froicu, S. Deng, W. D. Shlomchik, F. G. Lakkis, and D. M. Rothstein. 2011. Regulatory T cells require mammalian target of rapamycin signaling to maintain both homeostasis and alloantigen-driven proliferation in lymphocyte-replete mice. *J. Immunol.* 186: 2809–2818.
36. Shin, H. J., J. Baker, D. B. Leveson-Gower, A. T. Smith, E. I. Segal, and R. S. Negrin. 2011. Rapamycin and IL-2 reduce lethal acute graft-versus-host disease associated with increased expansion of donor type CD4+CD25+Foxp3+ regulatory T cells. *Blood* 118: 2342–2350.
37. Liesz, A., E. Suri-Payer, C. Veltkamp, H. Doerr, C. Sommer, S. Rivest, T. Giese, and R. Veltkamp. 2009. Regulatory T cells are key cerebroprotective immunomodulators in acute experimental stroke. *Nat. Med.* 15: 192–199.
38. Thornton, A. M., P. E. Korty, D. Q. Tran, E. A. Wohlfert, P. E. Murray, Y. Belkaid, and E. M. Shevach. 2010. Expression of Helios, an Ikaros transcription factor family member, differentiates thymic-derived from peripherally induced Foxp3+ T regulatory cells. *J. Immunol.* 184: 3433–3441.
39. Yilmaz, G., and D. N. Granger. 2010. Leukocyte recruitment and ischemic brain injury. *Neuromolecular Med.* 12: 193–204.
40. Wang, Q., X. N. Tang, and M. A. Yenari. 2007. The inflammatory response in stroke. *J. Neuroimmunol.* 184: 53–68.
41. Kleinschmitz, C., N. Schwab, P. Kraft, I. Hagedorn, A. Dreykluft, T. Schwarz, M. Austinat, B. Nieswandt, H. Wiendl, and G. Stoll. 2010. Early detrimental T-cell effects in experimental cerebral ischemia are neither related to adaptive immunity nor thrombus formation. *Blood* 115: 3835–3842.
42. Iadecola, C., and J. Anrather. 2011. The immunology of stroke: from mechanisms to translation. *Nat. Med.* 17: 796–808.
43. Kleinschmitz, C., P. Kraft, A. Dreykluft, I. Hagedorn, K. Göbel, M. K. Schuhmann, F. Langhauser, X. Helluy, T. Schwarz, S. Bittner, et al. 2013. Regulatory T cells are strong promoters of acute ischemic stroke in mice by inducing dysfunction of the cerebral microvasculature. *Blood* 121: 679–691.
44. Ren, X., K. Akiyoshi, A. A. Vandenbark, P. D. Hurn, and H. Offner. 2011. CD4+FoxP3+ regulatory T-cells in cerebral ischemic stroke. *Metab. Brain Dis.* 26: 87–90.
45. Wohler, J. E., S. S. Smith, K. R. Zinn, D. C. Bullard, and S. R. Barnum. 2009. Gamma delta T cells in EAE: early trafficking events and cytokine requirements. *Eur. J. Immunol.* 39: 1516–1526.
46. Lakhani, S. E., A. Kirchgesner, and M. Hofer. 2009. Inflammatory mechanisms in ischemic stroke: therapeutic approaches. *J. Transl. Med.* 7: 97.
47. Frenkel, D., Z. Huang, R. Maron, D. N. Koldzic, M. A. Moskowitz, and H. L. Weiner. 2005. Neuroprotection by IL-10-producing MOG CD4+ T cells following ischemic stroke. *J. Neurol. Sci.* 233: 125–132.
48. Strle, K., J. H. Zhou, W. H. Shen, S. R. Broussard, R. W. Johnson, G. G. Freund, R. Dantzer, and K. W. Kelley. 2001. Interleukin-10 in the brain. *Crit. Rev. Immunol.* 21: 427–449.
49. Lee, J. H., J. P. Lydon, and C. H. Kim. 2012. Progesterone suppresses the mTOR pathway and promotes generation of induced regulatory T cells with increased stability. *Eur. J. Immunol.* 42: 2683–2696.
50. Yurchenko, E., M. T. Shio, T. C. Huang, M. Da Silva Martins, M. Szyf, M. K. Levings, M. Olivier, and C. A. Piccirillo. 2012. Inflammation-driven reprogramming of CD4+ Foxp3+ regulatory T cells into pathogenic Th1/Th17 T effectors is abrogated by mTOR inhibition in vivo. *PLoS One* 7: e35572.
51. Battaglia, M., A. Stabilini, and E. Tresoldi. 2012. Expanding human T regulatory cells with the mTOR-inhibitor rapamycin. *Methods Mol. Biol.* 821: 279–293.
52. Delgoffe, G. M., T. P. Kole, Y. Zheng, P. E. Zarek, K. L. Matthews, B. Xiao, P. F. Worley, S. C. Kozma, and J. D. Powell. 2009. The mTOR kinase differentially regulates effector and regulatory T cell lineage commitment. *Immunity* 30: 832–844.
53. Zhang, P., S. K. Tey, M. Koyama, R. D. Kuns, S. D. Oliver, K. E. Lineburg, M. Lor, B. E. Teal, N. C. Raffelt, J. Raju, et al. 2013. Induced regulatory T cells promote tolerance when stabilized by rapamycin and IL-2 in vivo. *J. Immunol.* 191: 5291–5303.
54. Zhang, W., D. Zhang, M. Shen, Y. Liu, Y. Tian, A. W. Thomson, W. P. Lee, and X. X. Zheng. 2010. Combined administration of a mutant TGF-beta1/Fc and rapamycin promotes induction of regulatory T cells and islet allograft tolerance. *J. Immunol.* 185: 4750–4759.
55. Park, Y., H. S. Jin, J. Lopez, C. Elly, G. Kim, M. Murai, M. Kronenberg, and Y. C. Liu. 2013. TSC1 regulates the balance between effector and regulatory T cells. *J. Clin. Invest.* 123: 5165–5178.
56. Haxhinasto, S., D. Mathis, and C. Benoist. 2008. The AKT-mTOR axis regulates de novo differentiation of CD4+Foxp3+ cells. *J. Exp. Med.* 205: 565–574.
57. Collison, L. W., C. J. Workman, T. T. Kuo, K. Boyd, Y. Wang, K. M. Vignali, R. Cross, D. Sehry, R. S. Blumberg, and D. A. Vignali. 2007. The inhibitory cytokine IL-35 contributes to regulatory T-cell function. *Nature* 450: 566–569.

58. Tsuji-Takayama, K., M. Suzuki, M. Yamamoto, A. Harashima, A. Okochi, T. Otani, T. Inoue, A. Sugimoto, T. Toraya, M. Takeuchi, et al. 2008. The production of IL-10 by human regulatory T cells is enhanced by IL-2 through a STAT5-responsive intronic enhancer in the IL-10 locus. *J. Immunol.* 181: 3897–3905.
59. Tsuji-Takayama, K., M. Suzuki, M. Yamamoto, A. Harashima, A. Okochi, T. Otani, T. Inoue, A. Sugimoto, R. Motoda, F. Yamasaki, et al. 2008. IL-2 activation of STAT5 enhances production of IL-10 from human cytotoxic regulatory T cells, HOZOT. *Exp. Hematol.* 36: 181–192.
60. Brandenburg, S., T. Takahashi, M. de la Rosa, M. Janke, G. Karsten, T. Muzzulini, Z. Orinska, S. Bulfone-Paus, and A. Scheffold. 2008. IL-2 induces in vivo suppression by CD4(+)CD25(+)Foxp3(+) regulatory T cells. *Eur. J. Immunol.* 38: 1643–1653.
61. Dodge, I. L., G. Demirci, T. B. Strom, and X. C. Li. 2000. Rapamycin induces transforming growth factor-beta production by lymphocytes. *Transplantation* 70: 1104–1106.
62. Wang, X., W. Wang, J. Xu, J. Hong, and Q. Le. 2013. Pretreatment of rapamycin before allogeneic corneal transplant promotes graft survival through increasing CD4(+)CD25(+)Foxp3(+) regulatory T cells. *Exp. Clin. Transplant.* 11: 56–62.
63. Wang, C., T. Yi, L. Qin, R. A. Maldonado, U. H. von Andrian, S. Kulkarni, G. Tellides, and J. S. Pober. 2013. Rapamycin-treated human endothelial cells preferentially activate allogeneic regulatory T cells. *J. Clin. Invest.* 123: 1677–1693.
64. Turnquist, H. R., G. Raimondi, A. F. Zahorchak, R. T. Fischer, Z. Wang, and A. W. Thomson. 2007. Rapamycin-conditioned dendritic cells are poor stimulators of allogeneic CD4+ T cells, but enrich for antigen-specific Foxp3+ T regulatory cells and promote organ transplant tolerance. *J. Immunol.* 178: 7018–7031.
65. Hu, X., P. Li, Y. Guo, H. Wang, R. K. Leak, S. Chen, Y. Gao, and J. Chen. 2012. Microglia/macrophage polarization dynamics reveal novel mechanism of injury expansion after focal cerebral ischemia. *Stroke* 43: 3063–3070.
66. Perego, C., S. Fumagalli, and M. G. De Simoni. 2011. Temporal pattern of expression and colocalization of microglia/macrophage phenotype markers following brain ischemic injury in mice. *J. Neuroinflammation* 8: 174.
67. Lambertsen, K. L., K. Biber, and B. Finsen. 2012. Inflammatory cytokines in experimental and human stroke. *J. Cereb. Blood Flow Metab.* 32: 1677–1698.
68. Shih, A. Y., H. B. Fernandes, F. Y. Choi, M. G. Kozoriz, Y. Liu, P. Li, C. M. Cowan, and A. Klegeris. 2006. Policing the police: astrocytes modulate microglial activation. *J. Neurosci.* 26: 3887–3888.
69. Viscomi, M. T., M. D'Amelio, V. Cavallucci, L. Latini, E. Bisicchia, F. Nazio, F. Fanelli, M. Maccarrone, S. Moreno, F. Cecconi, and M. Molinari. 2012. Stimulation of autophagy by rapamycin protects neurons from remote degeneration after acute focal brain damage. *Autophagy* 8: 222–235.
70. Lisi, L., P. Navarra, D. L. Feinstein, and C. Dello Russo. 2011. The mTOR kinase inhibitor rapamycin decreases iNOS mRNA stability in astrocytes. *J. Neuroinflammation* 8: 1.
71. Codeluppi, S., C. I. Svensson, M. P. Hefferan, F. Valencia, M. D. Silldorff, M. Oshiro, M. Marsala, and E. B. Pasquale. 2009. The Rheb-mTOR pathway is upregulated in reactive astrocytes of the injured spinal cord. *J. Neurosci.* 29: 1093–1104.
72. Banerjee, S., S. M. Gianino, F. Gao, U. Christians, and D. H. Gutmann. 2011. Interpreting mammalian target of rapamycin and cell growth inhibition in a genetically engineered mouse model of Nf1-deficient astrocytes. *Mol. Cancer Ther.* 10: 279–291.